scientific reports

Check for updates

OPEN

Downregulation of E-cadherin in pluripotent stem cells triggers partial EMT

C. E. Aban, A. Lombardi, G. Neiman, M. C. Biani, A. La Greca, A. Waisman, L. N. Moro, G. Sevlever, S. Miriuka & C. Luzzani✉

Epithelial to mesenchymal transition (EMT) is a critical cellular process that has been well characterized during embryonic development and cancer metastasis and it also is implicated in several physiological and pathological events including embryonic stem cell differentiation. During early stages of differentiation, human embryonic stem cells pass through EMT where deeper morphological, molecular and biochemical changes occur. Though initially considered as a decision between two states, EMT process is now regarded as a fluid transition where cells exist on a spectrum of intermediate states. In this work, using a CRISPR interference system in human embryonic stem cells, we describe a molecular characterization of the effects of downregulation of E-cadherin, one of the main initiation events of EMT, as a unique start signal. Our results suggest that the decrease and delocalization of E-cadherin causes an incomplete EMT where cells retain their undifferentiated state while expressing several characteristics of a mesenchymal-like phenotype. Namely, we found that E-cadherin downregulation induces *SNAI1* and *SNAI2* upregulation, promotes *MALAT1* and *LINC-ROR* downregulation, modulates the expression of tight junction occludin 1 and gap junction connexin 43, increases human embryonic stem cells migratory capacity and delocalize β-catenin. Altogether, we believe our results provide a useful tool to model the molecular events of an unstable intermediate state and further identify multiple layers of molecular changes that occur during partial EMT.

Abbreviations

EMT	Epithelial to mesenchymal transition
hESC	Human embryonic stem cells
PSC	Pluripotent stem cells
Dox	Doxycycline

Human pluripotent stem cells have the unique capacity to differentiate into the three germinal layers of the embryo (mesoderm, endoderm and ectoderm) and can build up all cell lineages of the body. In fact, formation of the trilaminar embryonic disk requires sequential rounds of differentiation of these cells into different and specialized cell types[1] demonstrating their high versatility. In particular, human embryonic stem cells (hESC) are pluripotent stem cells (PSC) derived from the inner cell mass of blastocyst and are able to differentiate into diverse cellular types using known stimuli. Nowadays, differentiation of mesenchymal stem cells (MSC) from PSC represents a valuable strategy due to their relevant immunomodulatory properties and offers a renewable source of these cells. For this, several protocols and strategies have been established during the past years[2,3]. Clinical use of MSC impose a strong challenge to produce a large quantity of these cells in a short time. Significant efforts have been made to overcome these limitations. One strategy for this is to shorten differentiation times. In this sense, we believe that intervening during the first stages of PSC differentiation could accelerate this process.

PSC remain closely associated with neighboring stem cells growing in compact colonies. However, during early stages of differentiation, PSC undergo through an epithelial to mesenchymal transition (EMT) where deep morphological, molecular and biochemical changes occur[4,5]. EMT involves a series of events where epithelial cells lose their adhesion properties and acquire migratory capacity and other traits of a mesenchymal phenotype[1]. This biological process has been comprehensively characterized and its implicated in several physiological and pathological events including embryonic stem cell differentiation, tissue repair and acquisition of certain properties of cancer stem cells[6].

LIAN-CONICET, FLENI, Buenos Aires, Argentina. ✉email: cluzzani@fleni.org.ar

Hallmark changes of EMT include alterations in cytoskeleton architecture, acquisition of migratory capacity, loss of apico-basal polarity and loss of cell adhesion. This phenotypic switch is mediated by activation of master transcription factors of EMT including SNAI1, SNAI2 and ZEB1/2 whose functions are finely regulated at transcriptional and translational levels[7]. In line with this, initiation of EMT involves changes in gene expression and activation of signaling pathways[8]. Also, microRNAs, long noncoding RNAs and modification at post-translational levels are implicated in the regulation of this process[9]. However, one of the main initiation signals of EMT is downregulation of E-cadherin (CDH1), a homophilic protein that mediates attachment to neighboring cells through interaction of its extracellular domains. Its expression is decreased during EMT and loss of function of this protein promotes this transition. The transcriptional repression of E-cadherin has long been considered a critical step during EMT[10].

Initially, EMT was considered as a decision between either epithelial or mesenchymal states. Nowadays, it is well known that EMT is not a binary process and that it can be considered as a fluid transition where cells exist on a spectrum of intermediate states. During EMT, cells can adopt a hybrid and transient state called partial EMT phenotype[9]. Cells in partial EMT, also known as an incomplete EMT, have characteristics of both epithelial and mesenchymal phenotypes. These mixed traits enable cells to undergo collective cell migration instead of an individual cell migration occurring in mesenchymal cells[11,12]. Partial EMT has been usually labeled as a metastable and reversible state[12,13], which is determined by cell type and signals strength that initiate and maintain continuity of EMT process.

Until now, blockade of E-cadherin to interfere with EMT was performed using neutralizing antibodies and siRNAs. However, the use of more precise technologies and the ability to modify specific targets through the CRISPR-Cas9 system represent a more powerful tool to investigate molecular events of EMT. We believe that E-cadherin disruption could be used as a method to force the first steps of EMT and therefore generate improve the existing mesenchymal stem cells differentiation protocols. In this work we describe the molecular effects of E-cadherin downregulation in human embryonic stem cells, as a unique signal for inducing EMT. Our results suggest that induced decrease of E-cadherin expression by CRISPR interference system leads to partial EMT obtaining cells that conserve their pluripotency but also express characteristics of a mesenchymal-like phenotype.

Results

Characterization of HES3-KRAB^{CDH1} cells. EMT is a key biological process that occurs during embryogenesis, normal wound healing, and cancer metastasis. Accordingly, a plethora of stimuli can trigger this event and most of them converge in a downregulation of E-cadherin expression, a key process of EMT. To study whether downregulation of E-cadherin is sufficient to induce an EMT-like process we first generated a hESC line that represses this gene using a catalytically inactive CRISPR/Cas9 fused to a KRAB repressor domain inducible by Dox and a sgRNA targeting the *CDH1* promoter that encodes E-cadherin[14] (Fig. 1a). After establishing the clonal cell line named HES3-KRAB^{CDH1}, we validated its effectiveness. Expression of KRAB protein was evaluated by immunofluorescence after cells were incubated with Dox (500 nM) during 48, 72 and 96 h. Without Dox, cells did not express KRAB protein but after Dox addition, positive immunostaining of KRAB is detectable and increases gradually during incubation time (Fig. S1). Then, we analyzed the efficiency of transcriptional repression of this cell line. For this, the expression level of the E-cadherin gene (*CDH1*) was measured by qPCR after cells were incubated with Dox at different times. As soon as 48 h, E-cadherin mRNA levels decreased significantly but a further reduction was observed at 72 and 96 h, times at which E-cadherin levels showed a threefold reduction relative to control condition (Fig. 1b). Parental HES3 wild type cells displayed no changes in expression of this gene after Dox treatment (Fig. S2). Finally, we assessed the inducible repression of E-cadherin at protein level. In the absence of Dox, as expected, E-cadherin was mainly localized at the cell membrane (Fig. 1c, left panel). Upon Dox treatment, E-cadherin levels substantially decreased in a time-dependent manner, until its levels were almost undetectable at 96 h (Fig. 1c, right panel). Overall, these results demonstrate that this inducible hESC line efficiently downregulates E-cadherin both at transcriptional and protein level.

Analysis of intercellular junctions after E-cadherin downregulation. Considering the structural relevance of E-cadherin in cell structure, we next assessed whether changes in its expression levels could affect cell morphology. As shown in Fig. 2a, without Dox, cells retained their classical morphology of PSC, growing as small round and compact cells in colonies with well-defined edges. However, silencing of E-cadherin caused a gradual change to a spindle-like morphology and produced a clear alteration in cellular distribution since each cell became isolated from other neighboring cells, as can also be seen in the nuclear density in Fig. 1c. This was further confirmed by assessing F-actin distribution by Phalloidin staining. Figure 2a shows that actin cytoskeleton reorganization accompanies the morphological changes seen in the colony. All these morphological alterations were not detected in parental HES3 incubated with or without Dox (Fig. S3). Since major morphological changes were observed in cells incubated with Dox at 96 h, we decided to measure cell area, perimeter and circularity compared to control cells. Quantification of these parameters was performed by staining cell membranes with wheat germ agglutinin (WGA) followed by quantitative image analysis (Fig. 2b). Overall, values of cell area and perimeter were higher in cells cultured with Dox compared to cells without Dox (control condition). Moreover, when cultured with Dox, cells seem to abandon the typical round and symmetrical shape that characterize pluripotent stem cells. Thus, this data suggests that E-cadherin downregulation induces morphological changes on HES3-KRAB^{CDH1} cells.

First steps of EMT involve destabilization and disassembly of cell–cell contact complexes including desmosomes, adherens, tight and gap junctions. To explore the idea that morphological changes induced by E-cadherin downregulation could be related to disassembly mediated by transcriptional regulation of other junction structures, we evaluated mRNA levels of several genes that compose this complex. Reduction of E-cadherin

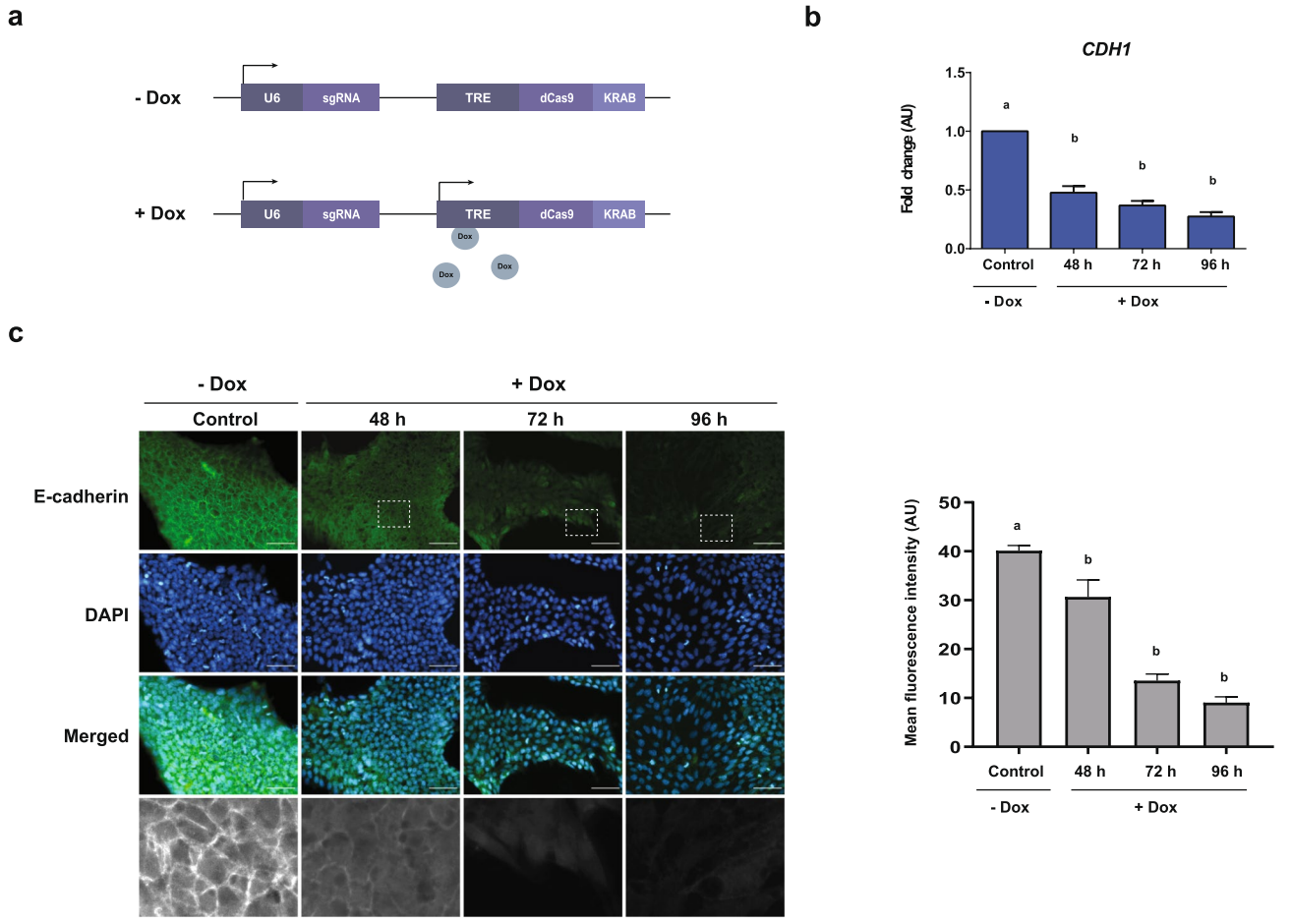

Figure 1. Characterization of HES3-KRAB^{CDH1} clonal cell line. (**a**) Schematic representation showing the construct used for generation of HES3-KRAB^{CDH1} cell line. This knockdown system contains a deactivated Cas9 (dCas9) fused to a transcriptional repressor domain Krüppel Associated Box (KRAB) under the control of TRE promoter inducible by Dox. A sgRNA against *CDH1* promoter was placed under the control of the U6 promoter which is constitutively activated. In cells not treated with Dox, the system is not active. Upon Dox induction, dCas9-KRAB is expressed and targeted to *CDH1* promoter by the sgRNA to produce transcriptional repression of E-cadherin. (**b**) Relative mRNA levels of E-cadherin (*CDH1*) in cells after incubation with Dox at different times assessed by qPCR. AU is the abbreviation for arbitrary units. Results are represented as mean ± SD (n = 5). Different letters indicate significant differences of groups compared to control condition ($p < 0.001$) for ANOVA with post hoc Tukey. (**c**) Left panel: immunofluorescence images of E-cadherin protein (green) in cells incubated with Dox during 48, 72 and 96 h. Nuclei were stained with DAPI (blue). Magnification of the indicated areas are shown in black and white at the bottom of the panel. Representative images of at least three experiments are shown. Scale bar 50 µm. Right panel quantification of the mean fluorescence intensity of three images from three independent experiments. Results are represented as mean ± SD (n = 3). Different letters indicate significant differences of groups compared to control condition ($p < 0.0001$) for ANOVA with post hoc Tukey.

did not induce any changes in the expression of genes involved in desmosome junctions such as desmoplakin (*DSP*), desmocollin (*DSC2*) and desmoglein (*DSG2*) (Fig. 2c). Also, no significant changes were observed in the expression of tight junction protein 1 (*TJP1*) and claudin 3 (*CLDN3*) two genes implicated in tight junctions (Fig. 2d). However, following E-cadherin downregulation, occludin 1 (*OCLN*), another gene implicated in this type of junction, showed a significant decrease. In the same line, expression of connexin-43 (*GJA1*), a primary component of gap junctions, also was significantly decreased compared to control condition (Fig. 2e). To further explore this, we compared the normalized mRNA levels of *CDH1*, *GJA1* and *OCLN* following Dox addition (Fig. 2f). Both the boxplot as well as Pearson's Correlation Analysis (PCA) showed a direct correlation in the decrease of *OCLN* and *GJA1* mRNA with E-cadherin downregulation, albeit this seems to be stronger between *CDH1* and *OCLN* (PCA = 0.78) than between *CDH1* and *GJA1* (PCA = 0.63). Together, this data demonstrated that expression of some components of intercellular junctions are modulated, suggesting that E-cadherin silencing could be inducing a partial alteration of genes related to the maintenance of cell structure.

E-cadherin silencing activate genes related to initiation of EMT. As our previous results suggested that E-cadherin downregulation induce some alterations that might be related to early stages of EMT, our aim was to evaluate if this decrease could initiate, activate and/or maintain this transition process. Hence, we first

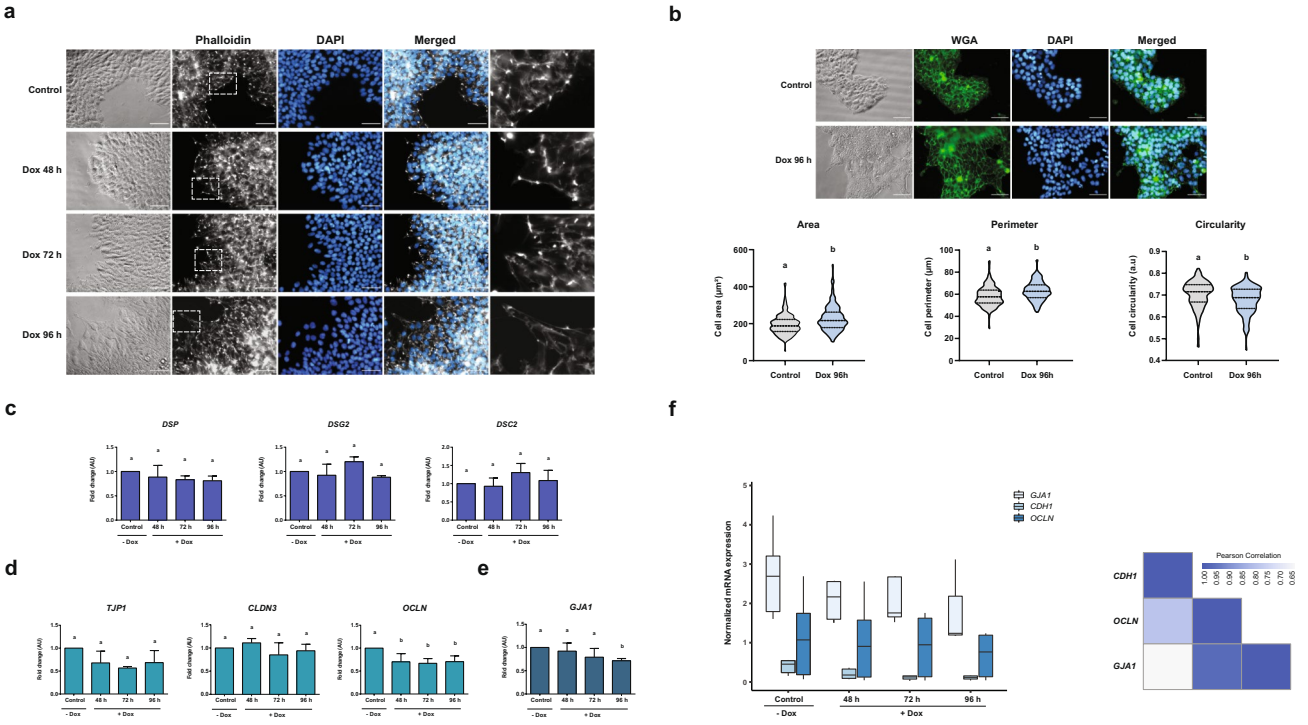

Figure 2. Downregulation of E-cadherin induced morphological alterations and transcriptional regulation of some adhesion complex genes. **a**) Morphological changes of HES3-KRAB^{CDH1} cells incubated with Dox at different times. Cells were stained with phalloidin (grey) to visualize F-actin and DAPI was used to stain the nucleus (blue). Magnifications of areas indicated by dotted lines are shown in the last column in black and white colors. Scale bar 50 µm. **b**) Cellular size and shape analysis of HES3-KRAB^{CDH1} cells. Cell membranes were defined by wheat germ agglutinin (WGA) labeling after incubation without Dox (Control) or with Dox during 96 h (96 h). Upper panel: representative images of cell membrane stained with WGA (green). Nucleus were stained with DAPI (blue). Scale bar 50 µm. Lower panel: graphical representation of quantification of cell area, perimeter and circularity. AU is the abbreviation for arbitrary units. (**c**) Relative mRNA expression of desmoplakin (*DSP*), desmoglein (*DSG2*), desmocollin (*DSC2*) (**d**) tight junction protein 1 (*TJP1*), claudin 3 (*CLDN3*), occludin 1 (*OCLN*) and (**e**) connexin 43 (*GJA1*), when E-cadherin is downregulated. AU is the abbreviation for arbitrary units. Results are represented as mean ± SD (n = 5). ANOVA with post hoc Tukey. Different letters indicate significant differences of groups compared to control condition ($p < 0.05$). (**f**) Left: normalized mRNA expression of E-cadherin (*CDH1*), occludin-1 (*OCLN*) and connexin 43 (*GJA1*) genes. Right: heat map showing Pearson's correlation coefficient between these genes.

analyzed if cells that sub-express E-cadherin retained an undifferentiated and pluripotent state. We found that E.cadherin downregulation did not alter the expression pattern of the pluripotency genes *OCT4* (*POU5F1*), *NANOG*, SOX2 and *LIN28* (*LIN28A*) (Fig. 3a,b). Although expression of *OCT4* mRNA shows a slight reduction at 72 h, this does not seem to have an impact on its protein at 96 h (Fig. 3b). Moreover, when Dox-treated cells were subjected to a non-directed differentiation protocol by embryoid bodies formation, markers for all three germ layers (i.e. *GATA4* for endoderm, *NKX2.5* for mesoderm and *TUBB3* for ectoderm) were expressed as shown in Fig. 3c. Overall, this data suggest that pluripotency of HES3-KRAB^{CDH1} cells is not affected by E-cadherin downregulation.

Then, we studied the genes involved in EMT, namely *SNAI1*, *SNAI2*, *ZEB1* and *ZEB2*, and the genes of early mesoderm precursor *TBX6, MIXL1* after Dox incubation and consequent E-cadherin decrease. Although gene expression of transcription factors ZEB1 and ZEB2, as well as early mesoderm genes did not present significant differences, we found that expression of *SNAI1* and *SNAI2*, two key master transcription factors in the initiation of EMT were significantly upregulated (Fig. 4a,b).

Activation of EMT occurs in response to various factors and signals. Different reports tend to focus on the study of long non-coding RNA (lncRNA) as fundamental regulators of EMT in cancer stem cells and PSC[15]. Based on this background, our next step consisted of evaluating the expression of *LINC-ROR* and *MALAT1*, two lncRNAs considered as EMT regulators, during E-cadherin downregulation. As observed in Fig. 4c, both lncRNAs were significantly downregulated in all experimental conditions. Another factor that contributes to EMT activation is β-catenin, a protein that interacts with the cytoplasmic domain of E-cadherin. When the latter is downregulated, β-catenin is released into the cytoplasm and can translocate into the nucleus[16], leading to transcriptional activation of genes related to EMT. In order to have an approximation about activation of this pathway, we evaluated localization of β-catenin after E-cadherin downregulation. Immunofluorescence showed that, in control conditions, β-catenin is present in the cytoplasmic compartment. Upon reduction of E-cadherin, we observed a marked decrease of this protein in the cytoplasm (Fig. 4d) and an accumulation in the center of the

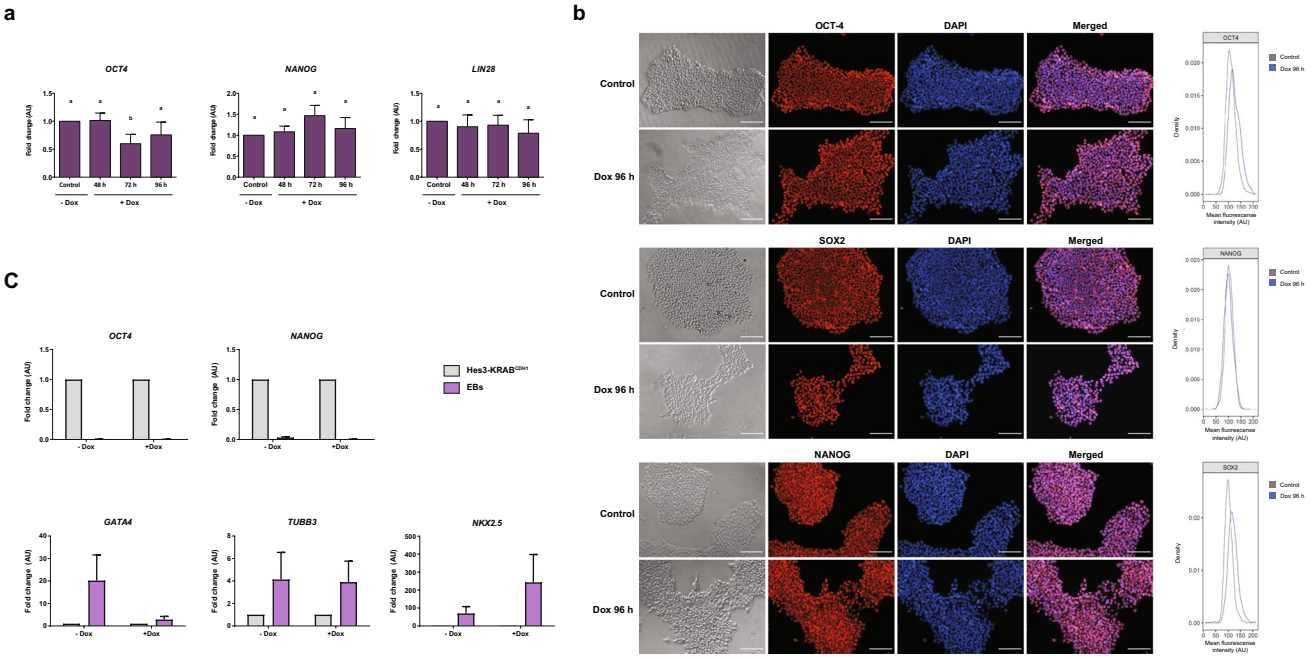

Figure 3. E-cadherin decrease does not modify pluripotency state. (**a**) qPCR analysis of pluripotency genes *OCT4*, *NANOG* and *LIN28* after Dox treatment of HES3-KRAB^{CDH1} cells at different times. AU is the abbreviation for arbitrary units. Results are represented as mean ± SD (n = 5). ANOVA with post hoc Tukey. Different letters indicate significant differences of groups compared to control condition ($p < 0.05$). (**b**) Immunofluorescence and quantification of mean fluorescence intensity of OCT-4 (upper panel), SOX2 (middle panel) and NANOG (lower panel) (red) in HES3-KRAB^{CDH1} cells. Nucleus were stained with DAPI (blue). Scale bar 100 µm. (**c**) Expression of *NANOG* and *OCT-4* (pluripotency genes), *GATA4* (endoderm gene), *NKX2.5* (mesoderm gene) and *TUBB3* (ectoderm gene) in HES3- KRAB^{CDH1} cells and embryoid bodies (EB) with or without Dox treatment for 96 h. AU is the abbreviation for arbitrary units. Results are represented as mean ± SD.

nuclear compartment. Notably, quantitative image analysis reveals a general decrease of β-catenin signal upon E-cadherin downregulation. To determine if β-catenin effectively translocated into the nucleus, we analyzed the expression of two target genes of β-catenin signaling pathway, cyclin D1 (*CCND1*) and c-myc (*MYCBP*) (Fig. 4e). Expression levels of both genes decreased at 48 and 72 h of Dox treatment but returned to basal levels at 96 h suggesting that β-catenin pathway was not particularly activated after E-cadherin silencing. All together, these results indicate that even though the β-catenin signaling pathway does not seem to be activated, E-cadherin downregulation could be triggering the initial steps of EMT.

Downregulation of E-cadherin induces a partial EMT state. Rather than a binary switch between two states, it is accepted that during EMT cells can transiently adopt different intermediate states collectively described as partial EMT. To test whether E-cadherin downregulation could be inducing a partial EMT state, some features of this particular state were analyzed. As previously observed, both 72 and 96 h of Dox treatment induced a pronounced decrease of E-cadherin. In view of this, we decided to evaluate functional effects of E-cadherin silencing regardless of incubation time. While transitioning, cells can attain a partial EMT phenotype that enables them to move collectively which is characteristic of this state. Thus, we next evaluated cell migratory capacity through a wound healing assay. For this, cells were treated with Dox during 72 h and then a scratch was performed. Parental HES3 wild type cells did not display any migratory difference upon Dox treatment, indicating that Dox treatment per se does not modify the migratory phenotype of cells (Fig. S4). Importantly, when we performed this experiment in HES3-KRAB^{CDH1} cells, we observed that Dox treatment induced a significant increase in wound closure, suggesting that downregulation of E-cadherin stimulated collective cell migration (Fig. 5a).

Hybrid phenotype of partial EMT is usually described as metastable and since acquisition of this state is transitory, cells can revert to a previous state leaving in evidence their high plasticity. As an approach to evaluate reversibility of partial EMT phenotype, we performed a rescue experiment where cells were treated with Dox for 96 h. Afterwards, Dox was removed and cells were maintained only with medium for another 96 h (4 days). When Dox was removed, both E-cadherin downregulation and increase in *SNAI1* expression were reversed (Fig. 5b). mRNA levels of E-cadherin returned slowly to the same levels of control conditions within two days of Dox removal. Moreover, *SNAI1* expression returns to control levels the following day after Dox removal. These findings indicate that the effect of E-cadherin silencing is reversible, showing flexibility and plasticity of cells in partial EMT.

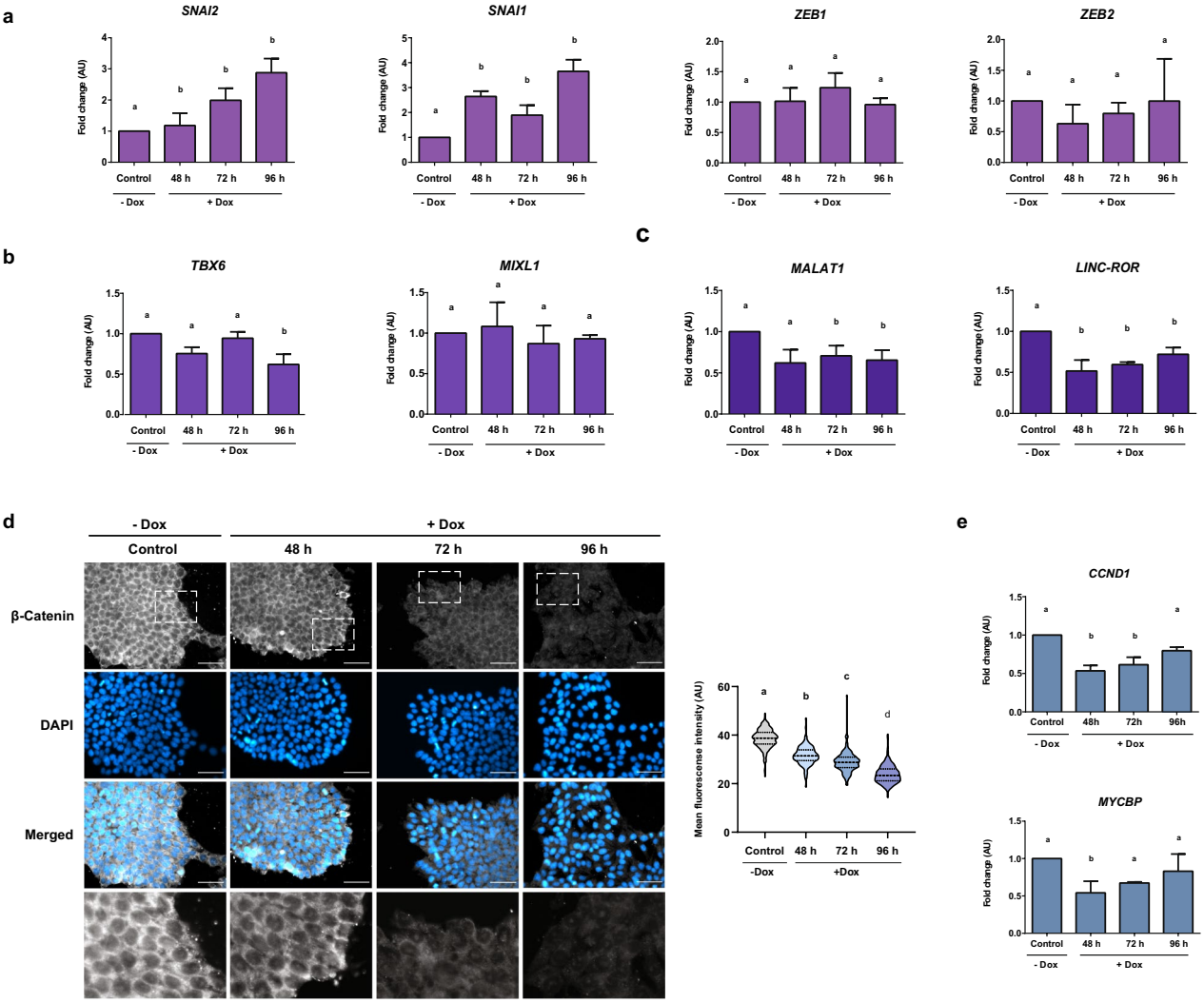

Figure 4. E-cadherin decrease activates the initiation of EMT. qPCR analysis of (**a**) genes involved in EMT such as *SNAI1*, *SNAI2*, *ZEB1* and *ZEB2* and (**b**) genes of early mesoderm precursor *TBX6* and *MIXL1* when E-cadherin is downregulated. (**c**) Relative expression level of *LINC-ROR* and *MALAT1*, two lnc-RNAs that act as regulators of EMT were measured by qPCR. AU is the abbreviation for arbitrary units. Results are represented as mean ± SD (n = 5). ANOVA with post hoc Tukey. Different letters indicate significant differences of groups compared to control condition ($p < 0.05$). (**d**) Immunofluorescence and quantification of mean fluorescence intensity of β-catenin (grey) in cells treated with Dox. Nuclei were stained with DAPI (blue). Magnification of dotted areas are shown in black and white colors. Scale bar 50 µm. Representative images of at least three experiments are shown. Results are represented as mean ± SD (n = 3). ANOVA with post hoc Tukey. Different letters indicate significant differences between groups ($p < 0.05$). (**e**) Relative mRNA levels of c-myc (*MYCBP*) and cyclin D1 (*CCND1*) were determined by qPCR. Data are presented as mean ± SD (n = 4). ANOVA with post hoc Tukey. Different letters indicate significant differences of groups compared to control condition ($p < 0.05$).

Discussion

EMT is a complex mechanism that involves morphological and molecular changes by which epithelial cells can acquire a mesenchymal phenotype. In this work we investigated the molecular effects of E-cadherin (CDH1) downregulation as a triggering signal for EMT activation in hESC. Overall, we found that this alteration induces a partial EMT where cells attain a hybrid state retaining their undifferentiated state while showing certain features of a mesenchymal-like phenotype.

In hESC, cell differentiation involves the loss of the undifferentiated state, activation of EMT and acquisition of a specific lineage. Molecular characterization of HES3-KRAB^{CDH1} following E-cadherin knockdown showed a slight disturbance in *OCT4* expression. A precise level of this gene must be sustained for the maintenance of pluripotency[17] and small variations could be related to this balance. However, no significant changes in *NANOG* and *LIN28* mRNA expression were observed. In addition, E-cadherin knockdown does not seem to alter OCT4, SOX and NANOG proteins nor the ability for the HES3-KRAB^{CDH1} to differentiate to the three germ layers. Altogether, our data suggest that the pluripotency of these cells was not disturbed by E-cadherin downregulation. However, E-cadherin silencing did induce a marked increase in *SNAI1* and *SNAI2* levels, alterations that were not observed in previous reports where E-cadherin abrogation in embryonic stem cells was evaluated[18]. Experimental

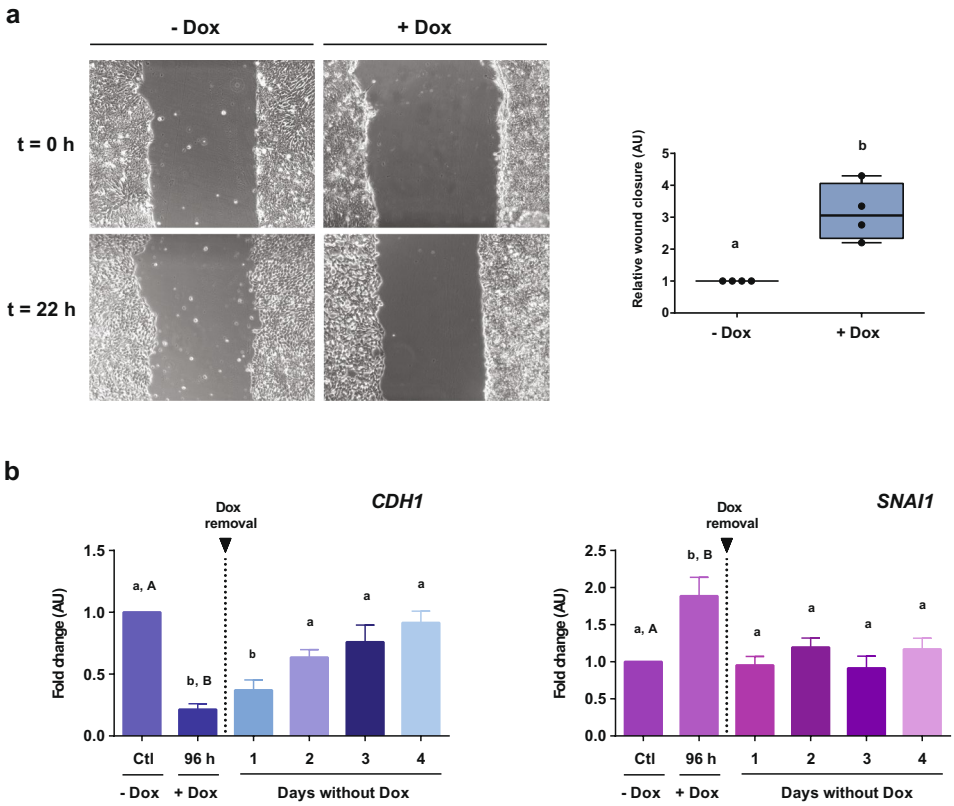

Figure 5. Silencing of E-cadherin induced a partial EMT state. (**a**) Wound healing assay was made after cells were treated with or without Dox (+Dox and −Dox, respectively) (t = 0 h). Cells were treated with Dox during 72 h and then scratch was made (t = 0 h for this experiment). Images were taken at t = 0 h and after 22 h of recovery (t = 22 h) (left). Graphic represents the relative wound closure area of at least four independent experiments (right). AU is the abbreviation for arbitrary units. T test. Different letters indicate significant differences. (**b**) Rescue experiment to regain the knockdown effect. Cells were incubated with Dox for 96 h. At this time point, Dox was removed and cells were maintained for another 96 h (4 days) only with culture medium. *CDH1* and *SNAI1* gene expression was evaluated by qPCR. Results are represented as mean ± SD (n = 5). AU is the abbreviation for arbitrary units. ANOVA with post hoc Tukey. Different letters indicate significant differences of groups compared to control condition ($p < 0.01$).

observations reported that SNAI1 is induced at the initiation of EMT whereas ZEB1 is produced at a lather phase. In fact, SNAI1 is proposed to trigger this process inducing a decrease in E-cadherin followed by a second step where ZEB1 further reinforces this effect[19–22]. These sequential steps are necessary for a complete EMT to occur. Induction of *SNAI1*, but not of *ZEB1* as observed in our results, suggest that E-cadherin partial downregulation does not have enough strength on its own to signal the next step of EMT resulting in an incomplete event. This could be explained by the regulation of *SNAI1* and E-cadherin expression. E-cadherin prevents stimulation of NF-Kappa-B and other signaling pathways, but when its levels are low this pathway is activated and acts as an inductor of *SNAI1* expression[23]. Moreover, *SNAI1* levels are amplified by a self-stimulatory loop resulting in higher levels of this gene which are necessary for activation of other transcriptional repressors of E-cadherin such as ZEB1[21]. Probably, in our system, partial E-cadherin downregulation did not induce an increase of *SNAI1* to the levels necessary to activate *ZEB1*, resulting in a partial EMT.

Currently there is no general agreement on the molecular markers that identify univocally cells in a partial EMT state. Currently, some reports have determined partial EMT state based on the detection of E-cadherin and vimentin[24], markers of epithelial and mesenchymal state, respectively. On the other hand, Puram et al.[25] analyzed a gene expression panel for features of EMT detecting an increased expression of TGF-β (a regulator of EMT) and vimentin while the expression of epithelial markers and other classical EMT transcription factors remain unaltered. In view of these findings, we considered a wide range of molecules and features of EMT to make a complete molecular characterization. Our results indicated that E-cadherin silencing in HES3-KRAB^{CDH1} cells caused a higher expression of EMT transcription factors genes *SNAI1* and *SNAI2*, an alteration of cell morphology to a mesenchymal-like phenotype and an enhanced collective cell migration. Notably, all these partial changes correspond to those observed during EMT. However, several other reports have shown that SNAI1 functions are not restricted only to EMT initiation. This transcription factor participates in all the events mentioned above, inducing morphological changes, regulating cell adhesion and partially modulating genes of tight junctions[26,27]. This suggests that SNAI1 also could be implicated in these alterations and in the acquisition of the incomplete EMT state.

Even though loss of E-cadherin is considered a hallmark event of EMT, many other signals and cellular events are required to activate this process. Up to recent years, lncRNAs has emerged as important regulators of several biological processes[15]. *LINC-ROR* is highly expressed in ESC and its implicated in the maintenance of pluripotency since act as sponge of microRNA that repress the translation of pluripotency genes, ensuring the undifferentiated state. When *LINC-ROR* expression decreases, synthesis of these pluripotent genes is repressed. However, a positive feedback loop of this pluripotency genes enables them to control and activate their own synthesis[28]. This autoregulatory circuitry provides a mechanism by which stem cells retain their ability to react appropriately to differentiation signals[29]. Our data suggest that although E-cadherin decrease down-regulated *LINC-ROR* levels, it does not have enough strength as an individual signal to induce a disturbance in pluripotency genes expression. On the other hand, β-catenin signaling is determined by its stabilization and accumulation in the cytoplasm[16]. In fact, a key step in the WNT pathway is regulation of β-catenin cytosolic pool which is available for nuclear translocation and activation of gene transcription[30]. A partial downregulation of E-cadherin as occurs in our system could involve lower free β-catenin levels than threshold levels necessary to translocate into the nucleus and activate this pathway.

In this work we could observe that low E-cadherin levels contribute to leave cells in a pre-differentiation state that could be more susceptible to external signals that follow up the complete transition event. As concluding remarks, recent experimental findings have bolstered the relevance of partial EMT until to be considered as a focal point of study in the EMT field. Due to their unstable nature, it has been extremely difficult to establish adequate models that enable to have a better understanding about this particular state. In this work, we could establish a model of partial EMT in hESC induced by downregulation of E-cadherin, a hallmark event of EMT. Moreover, this is the first time that this intermediary state is detected in PSC. We believe our results can be used as a platform to identify different aspects of this particular state and its impact in initial differentiation events. Results obtained here provide a useful tool that will allow us to investigate molecular events of an unstable intermediate state and identify multiple layers of molecular changes that occur during partial EMT.

Materials and methods

Embryonic stem cells culture. Human embryonic stem cells HES3 were generously donated by Edouard Stanley's Lab. Cells were maintained in an undifferentiated state under feeder-free conditions on GelTrex-coated plates (15 µg/mL) (Thermo Fisher Scientific, USA). Cells were fed daily with mTeSR medium (STEM CELL Technologies, Canada) and maintained at 37 °C in a humidified atmosphere with 5% CO_2 in air. When cells reached approximately 70–80% of confluence, colonies were dissociated using TrypLE 1x (Thermo Fisher Scientific, USA) and cells were seeded on new culture dishes previously coated with Geltrex in mTeSR medium (STEMCELL Technologies, Canada) containing ROCK Inhibitor (Y-27632, Tocris, UK).

For experiments, cells were seeded in mTeSR medium. Once cells attached to the plate (typically after 2 h), medium was changed and doxycycline (Dox) (Doxycycline hyclate, Sigma Aldrich, USA) was added. Cells were incubated with Dox during 48, 72 and 96 h and Dox was renewed daily with medium change. At each of the indicated time points, material was collected to be analyzed later.

Generation of stable cell line. For inducible *CDH1* (E-cadherin gene) downregulation, a stable cell line called HES3-KRAB^{CDH1} was generated using the CRISPR interference system. To achieve this, a sgRNA directed to the promotor (200 bp upstream of transcription start site) of *CDH1* was cloned into the pLenti SpBsmBI sgRNA Puro plasmid (Addgene plasmid #62207) and used to generate non-replicative lentiviral particles, as previously described by Neiman et al.[31]. Sequences of sgRNA are listed in supplemental material (Table S1). Briefly, HEK293FT cells were co-transfected with sgRNA and lentiviral packaging plasmids and viral supernatants were collected at 48 h. Parental HES3 cells that express TRE-dCas9-KRAB construct[31] were dissociated to single cells with TrypLE and seeded at low density in mTser medium on GelTrex coated 6-well plates. On the following day, viral supernatant was added to the culture medium for 48 h. Then, medium was replenished and cells were treated with 1 µg/mL puromycin for 2 days. After selection, clonal isolation was performed. For this, 1 µL of a highly diluted cell suspension was plated in a 6-well plate and single cells were incubated with ROCK inhibitor (Y-26732) until they could form small colonies. After 7 days, individual colonies were hand-picked into 24 well plates and treated with 500 ng/mL of Dox to induce KRAB expression and E-cadherin repression. Cells were PCR genotyped for dCas9-KRAB and E-cadherin. Primer sequences are detailed in Table S2 (supplementary material).

Embryoid bodies differentiation. HES3-KRAB^{CDH1} cells were differentiated using the hanging drop method. Briefly, after 96 h with or without Dox, cells were trypsinized, centrifuged, and suspended in differentiation medium (standard medium containing 20% FSB) to a concentration of 25,000 cells/mL. Afterward, 25-mL drops were placed on the lid of a bacterial plate. After 48 h, EBs formed in the bottom of the drops were collected and placed in new bacterial plates with fresh differentiation medium, allowing them to grow for 3 more days. On the fifth day, EBs were collected and re-plated onto GelTrex-coated dishes. From the sixth day onward, adherent EBs were cultured until day 21.

Statement. For human experiments informed consent was obtained from all participants. All experiments and methods were performed in accordance with relevant guidelines and regulations. All experimental protocols were approved by FLENI Ethics Committee.

Immunofluorescence staining. Cells were seeded on coverslips coated with GelTrex in 24 well-plate and treated with Dox at different times. Then cells were fixed with 4% paraformaldehyde for 30 min, washed three

times with PBS (Sigma Aldrich, USA) and blocked for 45 min with 0,1% Triton X-100 (Sigma Aldrich, USA), 0,1% bovine serum albumin (BSA, Gibco, USA) and 10% Normal Goat Serum (Gibco, USA) in PBS at room temperature. Then, cells were washed twice with PBS for 5 min and incubated with specific primary antibodies overnight at 4 °C. The following day, cells were washed three times for 5 min and incubation with Alexa-fluor-conjugated secondary antibodies (Alexa 488 and Alexa 594, Life Technologies, USA) was performed for 1 h in a dark humid chamber. After that, cells were washed three times for 5 min with PBST (PBS + 0.1% Triton X-100). Nucleus were counterstained with DAPI for 15 min. Finally, cells were mounted on glass slides and examined by fluorescence microscopy on an EVOS Digital Color Fluorescence Microscope (Thermo Fisher Scientific, USA). Primary antibodies used in this work include anti-CDH1 (1:400, Clone 36/E-cadherin; Cat 612131, BD Biosciences, USA), anti- HA-tag for KRAB protein (1:500, 5B1D10, Cat 32-6700, Invitrogen, USA) and anti-β-Catenin (1:400, 4D5, Cat MA5-15569, Invitrogen, USA), anti-OCT-4 (1:200, C30A3C1, Cat 5677X, Cell Signaling), anti-NANOG (1:200, D73G4, Cat 5232X, Cell Signaling), anti-SOX2, D6D9, Cat 3579S, Cell Signaling).

For Phalloidin and WGA (Wheat Germ Agglutinin) staining, cells were seeded in a 48 well-plate and treated with Dox for different times. For Phalloidin staining, cells were fixed with 4% paraformaldehyde for 30 min, washed three times with PBS (Sigma Aldrich, USA) and stained with Texas Red-X phalloidin (165 nM, Cat T7471, Invitrogen) for 30 min. Then cells were washed 3 times with PBS (Sigma Aldrich, USA) and stained with DAPI for 15 min. WGA (Wheat Germ Agglutinin) staining was performed on live cells. Briefly, WGA (1 µg/mL, Cat W11261, Invitrogen) was added to the culture medium and incubated at 37 °C for 15 min, cells were washed 3 times with PSB (Sigma Aldrich, USA) and fixed with 4% paraformaldehyde for 30 min. Cells were washed with PBS (Sigma Aldrich, USA) 3 times and nucleus were counterstained with DAPI for 15 min. Finally, cells were examined by fluorescence microscopy on an EVOS Digital Color Fluorescence Microscope (Thermo Fisher Scientific, USA).

Quantitative qPCR analysis. Total RNA was isolated using Trizol Reagent (Invitrogen) according to manufacturer instructions and reverse-transcribed using M-MLV Reverse Transcriptase (Promega, USA). cDNA was amplified by qPCR with FastStart Universal SYBR Green Master reaction mix (Roche, Thermo Fisher Scientific, IN, USA) using specific primers detailed in Table S2 (supplementary material). qPCR was performed using a StepOnePlus Real Time PCR System (Applied Biosystems, USA) and analyzed using LinReg Software. All gene expression results were normalized to the geometric mean of RPL7 and HPRT1 housekeeping genes for each condition. Gene expression was analyzed by technical duplicates using at least three independent biological replicates.

Wound healing assay. Cells were seeded at low confluence in a 24 well-plate. After different days of Dox treatment, when cells reach 100% confluence, scratch wound healing assay was performed. Confluent monolayer was scratched with a sterile p200 pipette tip and immediately, cells were washed twice with PBS and fresh medium with Dox was added. Images were acquired at 0 and 22 h after injury via EVOS microscope (Life Technologies, USA). Experiments were performed at least three times. Quantification of the covered area was done by ImageJ software.

Quantification of cell area, perimeter, and circularity. Fluorescence images of WGA-stained (Wheat Germ Agglutinin) cells were acquired with EVOS microscopy (Thermos Fisher Scientific, USA). Images of three independent experiments were evaluated for each condition (control without Dox and Dox treatment at 96 h). The Cellpose segmentation algorithm[32] was used to create a mask where each cell is individually delineated. This mask was then used to quantify the area, perimeter and circularity of each cell using the ImageJ-FIJI software.

Statistical analysis. Results were expressed as mean ± SD of at least three biological replicates. Statistical significance was determined using t test and ANOVA. Comparison of means between groups was assessed using Tukey test. Residual fitted normal distribution and homogeneity of variance. Statistical differences were referred to control conditions. Results were considered significant when $p < 0.05$.

Received: 27 July 2020; Accepted: 11 January 2021
Published online: 21 January 2021

References

1. Kim, D. *et al.* Epitelial mesenchymal transition in embryonic development, tissue repair and cancer: A comprehensive overview. *J. Clin. Med.* **7**, 1 (2017).
2. Luzzani, C. D. & Miriuka, S. G. Pluripotent stem cells as a robust source of mesenchymal stem cells. *Stem Cell Rev. Rep.* **13**, 68–78 (2017).
3. Steens, J. & Klein, D. Current strategies to generate human mesenchymal stem cells in vitro. *Stem Cells Int.* **2018**, 1–10 (2018).
4. Eastham, A. M. *et al.* Epithelial–mesenchymal transition events during human embryonic stem cell differentiation. *Cancer Res.* **67**, 11254–11262 (2007).
5. Ullmann, U. *et al.* Epithelial–mesenchymal transition process in human embryonic stem cells cultured in feeder-free conditions. *Mol. Hum. Reprod.* **13**, 21–32 (2007).
6. Thiery, J. P., Acloque, H., Huang, R. Y. J. & Nieto, M. A. Epithelial–mesenchymal transitions in development and disease. *Cell* **139**, 871–890 (2009).
7. Lamouille, S., Xu, J. & Derynck, R. Molecular mechanisms of epithelial–mesenchymal transition. *Nat. Rev. Mol. Cell Biol.* **15**, 178–196 (2014).

8. Gonzalez, D. M. & Medici, D. Signaling mechanisms of the epithelial–mesenchymal transition. *Sci. Signal.* **7**, re8 (2014).
9. Sha, Y. *et al.* Intermediate cell states in epithelial-to-mesenchymal transition. *Phys. Biol.* **16**, 1–12 (2019).
10. Acloque, H., Adams, M. S., Fishwick, K., Bronner-Fraser, M. & Nieto, M. A. Epithelial–mesenchymal transitions: The importance of changing cell state in development and disease. *J. Clin. Investig.* **119**, 1438–1449 (2009).
11. Friedl, P. & Gilmour, D. Collective cell migration in morphogenesis, regeneration and cancer. *Nat. Rev. Mol. Cell Biol.* **10**, 445–457 (2009).
12. Jolly, M. K. *et al.* Implications of the hybrid epithelial/mesenchymal phenotype in metastasis. *Front. Oncol.* **5**, 1–19 (2015).
13. Hudson, L. G. *et al.* Cutaneous wound reepithelialization is compromised in mice lacking functional Slug (Snai2). *J. Dermatol. Sci.* **56**, 19–26 (2009).
14. Van Ijcken, W. F. J. *et al.* Eukaryotic transcriptional and post-transcriptional gene expression regulation. *Methods Mol. Biol.* **1507**, 129–140 (2017).
15. Gugnoni, M. & Ciarrocchi, A. Long noncoding RNA and epithelial mesenchymal transition in cancer. *Int. J. Mol. Sci.* **20**, 1–25 (2019).
16. Nelson, W. J. & Nusse, R. Convergence of Wnt, β-Catenin, and Cadherin pathways. *Science* **303**, 1483–1487 (2004).
17. Kashyap, V. *et al.* Regulation of stem cell pluripotency and differentiation involves a mutual regulatory circuit of the Nanog, OCT4, and SOX2 pluripotency transcription factors with polycomb repressive complexes and stem cell microRNAs. *Stem Cells Dev.* **18**, 1093–1108 (2009).
18. Ward, C. M., Mohamet, L. & Hawkins, K. Loss of function of E-cadherin in embryonic stem cells and the relevance to models of tumorigenesis. *J. Oncol.* **2011**, 20 (2011).
19. Thiery, J. P. & Sleeman, J. P. Complex networks orchestrate epithelial–mesenchymal transitions. *Nat. Rev. Mol. Cell Biol.* **7**, 131–142 (2006).
20. Peinado, H., Olmeda, D. & Cano, A. Snail, ZEB and bHLH factors in tumour progression: An alliance against the epithelial phenotype?. *Nat. Rev. Cancer* **7**, 415–428 (2007).
21. De Herreros, A. G., Peiró, S., Nassour, M. & Savagner, P. Snail family regulation and epithelial mesenchymal transitions in breast cancer progression. *J. Mammary Gland Biol. Neoplasia* **15**, 135–147 (2010).
22. Zhang, J. *et al.* TGF-β-induced epithelial-to-mesenchymal transition proceeds through stepwise activation of multiple feedback loops. *Sci. Signal.* **7**, ra91 (2014).
23. Julien, S. *et al.* Activation of NF-κB by Akt upregulates Snail expression and induces epithelium mesenchyme transition. *Oncogene* **26**, 7445–7456 (2007).
24. Jolly, M. K. *et al.* Stability of the hybrid epithelial/mesenchymal phenotype. *Oncotarget* **7**, 27067–27084 (2016).
25. Puram, S. V. *et al.* Single-cell transcriptomic analysis of primary and metastatic tumor ecosystems in head and neck cancer. *Cell* **171**, 1611-1624.e24 (2017).
26. Ohkubo, T. & Ozawa, M. The transcription factor Snail downregulates the tight junction components independently of E-cadherin downregulation. *J. Cell Sci.* **117**, 1675–1685 (2004).
27. Barrallo-Gimeno, A. & Nieto, M. A. The Snail genes as inducers of cell movement and survival: Implications in development and cancer. *Development* **132**, 3151–3161 (2005).
28. Fatica, A. & Bozzoni, I. Long non-coding RNAs: New players in cell differentiation and development. *Nat. Rev. Genet.* **15**, 7–21 (2014).
29. Boyer, L. A. *et al.* Core transcriptional regulatory circuitry in human embryonic stem cells. *Cell* **122**, 947–956 (2005).
30. Howard, S., Deroo, T., Fujita, Y. & Itasaki, N. A positive role of cadherin in wnt/β-catenin signalling during epithelial-mesenchymal transition. *PLoS One* **6**, 20 (2011).
31. Neiman, G. *et al.* Integrin alpha-5 subunit is critical for the early stages of human pluripotent stem cell cardiac differentiation. *Sci. Rep.* **9**, 18077 (2019).
32. Stringer, C., Wang, T., Michaelos, M. & Pachitariu, M. Cellpose : A generalist algorithm for cellular segmentation. 1–19 (2020).

Acknowledgements

We would like to thank Fleni Institute-CONICET and Pérez Companc Foundation for their continuous support.

Author contributions

C.E.A. carried out data collection, data analysis and writing of the original draft, A.L., contribute with data collection, analysis and interpretation of data, writing and critical revision of the article, G.N., M.C.B., A.L.G., A.W. and L.N.M., contributed to the interpretation of the results and critical revision of the manuscript, C.L. devised the project and design the study and assisted with drafting and critical revision of the manuscript. G.S., S.M. and C.L. conceived the original idea and helped supervise the project. All authors discussed the results and contributed to the final manuscript.

Funding

This work was supported by Grants from the National Agency for Scientific and Technical Promotion (ANPCyT) and from the Scientific and Technical Research Fund (FONCyT) PICT-2015-0868.

Competing interests

The authors declare no competing interests.

Additional information

Supplementary Information The online version contains supplementary material available at https://doi.org/10.1038/s41598-021-81735-1.

Correspondence and requests for materials should be addressed to C.L.

Reprints and permissions information is available at www.nature.com/reprints.

Publisher's note Springer Nature remains neutral with regard to jurisdictional claims in published maps and institutional affiliations.